NATIONAL INSTITUTE OF PUBLIC HEALTH AND THE ENVIRONMENT
BILTHOVEN, THE NETHERLANDS

RIVM report 658603 008

A PBPK-model for B(a)P in the rat relating dose and liver DNA-adduct level

M.J. Zeilmaker, J.C.H. van Eijkeren, M. Olling

April 1999

This investigation has been performed by order and for the account of the General Inspectorate for Health Protection within the framework of project 658603, chronic carcinogenity study with benzo(a)pyrene in the rat.

National Institute of Public Health and the Environment (RIVM), P.O. Box 1,
3720 BA Bilthoven, The Netherlands
Telephone: +31 - 30 - 274 91 11, telefax: +31 - 30 - 274 29 71

MAILING LIST

1 Hoofdinspecteur voor de Gezondheidsbescherming
2 Directeur Generaal Volksgezondheid
3 Plv. Directeur Generaal Volksgezondheid
4 Hoofdinspecteur Gezondheidszorg
5 Dr.ir. P.C. Bragt, IGB, Min. van VWS
6 Dr. M.E. Andersen, ICF Kaiser Engineeers, Research Triangle Park, USA
7 Dr. R. Conolly, Central Institute of Industrial Toxicology, Research Triangle Park, USA
8 Dr. P. Doucet, Vakgroep Theoretische Biologie, VU Amsterdam
9 Prof. Dr. W. Seinen, RITOX, Rijksuniversiteit Utrecht
10 Depot Nederlandse Publicaties en Nederlandse Bibliografie
11 Directie RIVM
12 Dr. Ir. H.J.G.M. Derks, Hoofd LGO
13 Dr.Ir. E. Lebret, Hoofd LBM
14 Dr. Ir. G. de Mik, Directeur Sector 4
15 Dr. A. Operhuizen, Hoofd LEO
16 Dr. W. Slob, LEO
17 Dr. M.P. van Veen, LBM
18 SBD/Voorlichting en Public Relations
19 Bibliotheek RIVM
20 Bureau Rapportenregistratie
21-23 Auteurs
24 Archief LBM
25-45 Bureau Rapportenbeheer

CONTENTS

Summary 4
Samenvatting 5

1. Introduction 6

2. PBPK model for B(a)P and its calibration 8
2.1 Model scheme 8
2.2 Model parametrization 9
2.3 Model calibration: RIVM studies in the rat 10

3. Rat PBPK model simulations and extrapolation to man 20
3.1 Dose dependency in the rat 20
3.2 Extrapolation to man 24

4. Conclusions 25

5. Literature 27

SUMMARY

In Olling *et al.* (1995) an experiment was reported about the toxicokinetics of Benzo-a-Pyrene (B(a)P) in rats after repeated daily dosing *p.o.* From this experiment it appeared that the kinetic parameters AUC, C_{max} and t_{max} varied as a function of time. For example, AUC and C_{max} were decreased on day 5 and 12 of the experiment with respect to their values on the first day, while on day 15, after the weekend during which no B(a)P was administered, these values returned almost to the values on day one.

In Zeilmaker *et al.* (1997[a]) a cellular model is reported about Ah-receptor dependent P450 induction by TetraChloroDibenzo-*p*-Dioxin (TCDD) and its consequential storage and metabolism in the rat liver. This cellular model was incorporated in a PBPK model of the rat. The PBPK model is generic in the sense that it can describe toxicokinetics of all kinds of lipophilic environmental contaminants, such as B(a)P.

In this report it is tried to explain the experimental observations of Olling *et al.* by the application of the model concepts of Zeilmaker *et al.* (1997) in a PBPK model for B(a)P in the rat. As in this model there is no time-dependency with respect to the absorption kinetic parameters, the only explanation for the observed reduction of the AUC and C_{max} that can be found is the auto-induced metabolism of B(a)P. As the absorption parameters in the model do not depend on time, the variation of t_{max} could not be explained.

With the calibrated B(a)P PBPK model for the rat simulations were performed. From these simulations the relation between dose level and internal concentrations of B(a)P and its metabolites could be found, as well as the relation between dose level and P450 enzymes induction status, EROD activity and DNA-adduct levels. It appears that the major fraction of metabolites is formed by the P450-1A2 enzyme. However, the minor fraction, formed by the P450-1A1 enzyme, seems only to be responsible for the formation of DNA-adducts.

SAMENVATTING

In Olling *et al.* (1995) wordt gerapporteerd over een experiment met betrekking tot de toxicokinetiek van Benzo-a-Pyreen (B(a)P) in ratten na herhaalde dagelijkse orale dosering. Uit dit experiment bleek dat de kinetische parameters AUC, C_{max} en t_{max} varieerden als functie van de dag van toediening. Op dag 5 en 12 van het experiment bijvoorbeeld waren AUC en C_{max} lager dan op dag een, terwijl op dag 15, na het weekend gedurende welke geen B(a)P werd toegediend, parameters weer bijna terug op het niveau van dag een waren.

In Zeilmaker *et al.* (1997) wordt een PBPK model geïntroduceerd over Ah-receptor afhankelijke inductie van P450-enzymen en de daaruit voortvloeiende geïnduceerde opslag en het geïnduceerde metabolisme in de rattelever van TCDD. Dit model kan aangewend worden voor allerlei lipofiele milieucontaminanten, zoals B(a)P.

In dit rapport wordt een gedeelte van de observaties uit Olling *et al.* verklaard met een PBPK model voor B(a)P in de rat volgens de concepten in Zeilmaker *et al.* (1997). Dit model bevat geen tijdsafhankelijkheid van absorptieparameters en de variatie van t_{max} kan er dus niet mee verklaard worden.

Met het gecalibreerde model zijn simulaties uitgevoerd die de vraag beantwoorden over de relatie tussen dosisniveau en de interne concentratie van moederstof en metabolieten, en over de relatie tussen dosisniveau en P450-enzym inductiestatus, EROD activiteit en DNA-adduct niveau. Deze blijken alle niet-lineair af te hangen van de dosis. Het DNA-adduct niveau evenwel blijkt lineair af te hangen van de door het P450 1A1-enzym gevormde metabolietconcentratie. Deze metaboliet vormt een mineure fractie van het totaal aan door het 1A2-enzym gevormde metabolieten.

1. INTRODUCTION

In M. Olling *et al.* (1995) an experiment was reported about the toxicokinetics of Benzo-a-Pyrene B(a)P in rats after repeated daily dosing *p.o.* From this experiment it appeared that the kinetic parameters AUC (area under the concentration-time curve), C_{max} (maximum reached concentration) and t_{max} (time point of reach of maximum concentration) varied as a function of time. At the first day of the experiment the values for AUC and C_{max} were maximal, while the value for t_{max} was minimal. At day 5 and day 12, i.e. the fifth day of the first and second week, AUC and C_{max} were minimal and t_{max} was maximal. However, at day 15, i.e. the first day after the weekend, during which the animals were not dosed, the values were intermediate and almost restored to the values at day 1. As far as the decrease in AUC and C_{max} after repeated dosing concerns, this can be explained by the phenomenon of auto-induction of the metabolism of B(a)P. This induction however, would lead to a greater metabolism rate, which would reduce t_{max}, instead of increasing it. Another explanation could be found in a slower absorption rate, by some unknown mechanism, perhaps caused by repeated dosing, together with a reduction of the bioavailable fraction. Of course, a combination of both could also be possible.

In Zeilmaker *et al.* (1997) a cellular model was reported about Ah-receptor dependent P450 induction by TetraChloroDibenzo-*p*-Dioxin (TCDD). This model was incorporated in a Physiologically Based PharmacoKinetic (PBPK) model of the rat. The PBPK model was calibrated on fixed dose/varying time-data from Abraham *et al.* (1988) and could well explain extra storage capacity of the rat liver together with induced metabolism. It was successfully applied in simulating varying dose/fixed-time data from *ibid.* and also in simulating data from Tritcher *et al.* (1992) and Kociba *et al.* (1978). This model is generic in the sense that it can be applied to all kinds of lipophilic environmental contaminants, such as B(a)P, that induce P450 enzymes.

In this report it is tried to explain the experimental observations of Olling *et al.* (1995) by the application of the model concepts of M. Zeilmaker *et al.* (1997) in a PBPK model for B(a)P in the rat. As in this model there is no time-dependency with respect to the absorption kinetic parameters, the only explanation for the observed reduction of the AUC and C_{max} that will be found is the auto-induced metabolism of B(a)P. The increase of t_{max} will not be explained by the model.

Based on the calibrated B(a)P model for the rat, the following questions will be raised within the frame of model concept and parametrization, assuming a daily oral dosing regime:

- what is the relation between dose level and "steady state" $C_{B(a)P,max}$, daily $AUC_{B(a)P}$, $C_{Met,max}$, daily AUC_{Met}. Here "Met" stands for metabolized B(a)P. N.b: B(a)P disappears so fast that dosing only once a day cannot lead to a steady state B(a)P concentration plateau
- will a steady state P450 enzyme concentration plateau be reached and consequently a plateau of EROD induction, and if so, what is the relation between these levels and B(a)P dose level
- can a relation be found between the formation of metabolites and the formation of specific DNA-adducts
- to extrapolate the PBPK model from a rat to a human model

In chapter two the concept model will be introduced, together with parameter calibration to the data. In the next chapter the above questions are answered by model simulations. The final chapter will contain some conclusions and remarks on the findings in the previous chapters.

2. PBPK MODEL FOR B(A)P AND ITS CALIBRATION

2.1. Model scheme

In Zeilmaker *et al.* (1997) a PBPK model for TCDD in the rat is developed. Essentially the same model has been used for B(a)P. The model scheme is depicted in Figure 1. For further reference and model equations, see *ibid.*

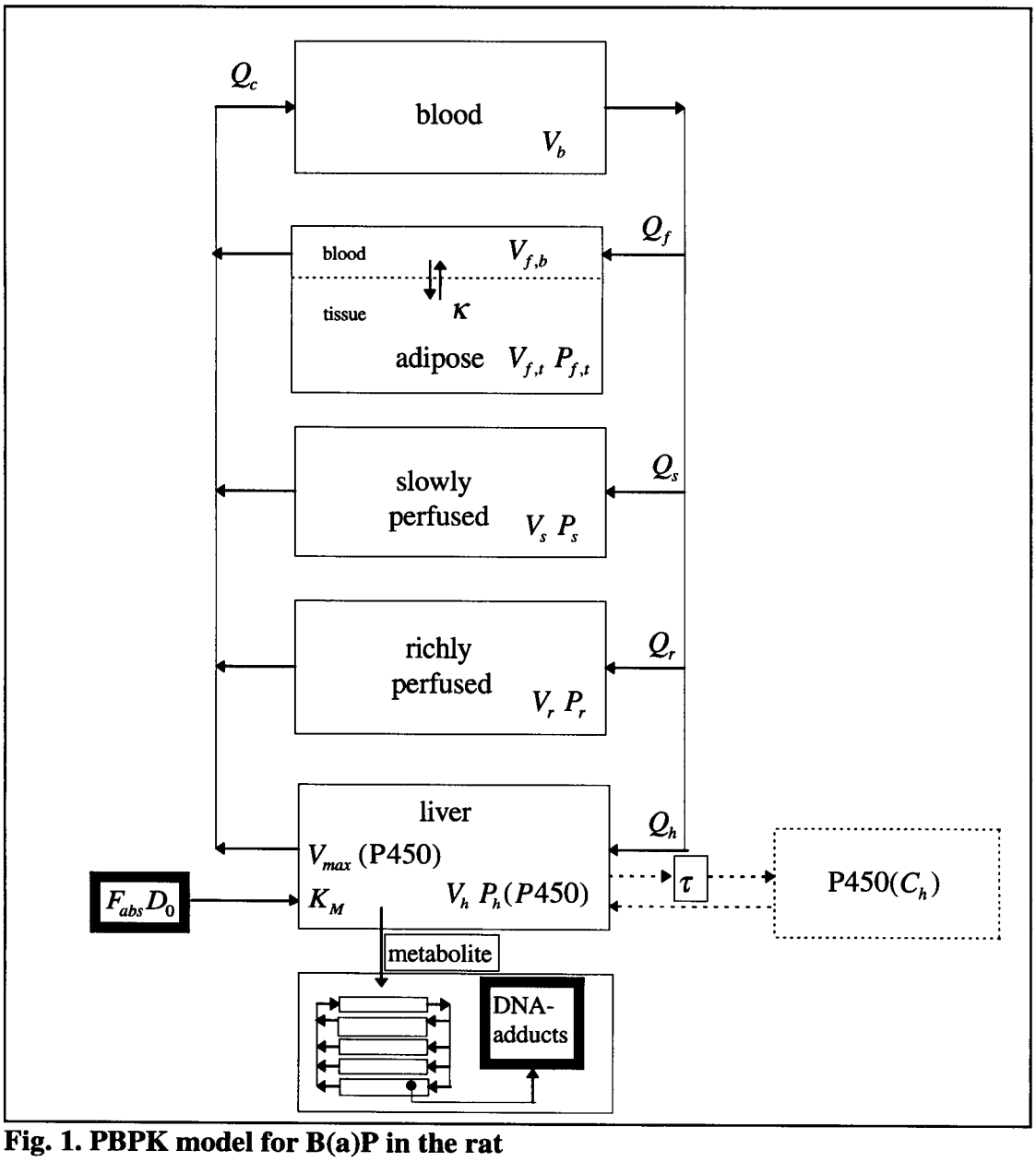

Fig. 1. PBPK model for B(a)P in the rat

Q: blood flow; V: volume; P: partition coefficient; C: concentration; P450: enzyme D_0: administered amount; F_{abs}: fraction absorbed over the gut wall; V_{max}: maximum possible metabolic rate; K_M: Michaelis-Menten constant; τ: time delay; κ: intra-compartmental diffusion; *b*: blood; *f*: fat; *s*: slowly perfused; *r*: richly perfused; *h*: hepatic

The solid lines in Figure 1 represent material flow of B(a)P by the blood flows through the compartments. The upper dotted arrow represents immaterial flow from the liver to a P450 compartment, i.e., the induction of P450 enzymes mediated by the B(a)P-Ah-receptor ligand, delayed by a time lag τ. The lower dotted arrow represents immaterial flow from the P450 compartment to the liver, i.e., the instantaneous enzyme induced storage, P_h, and metabolic capacity, V_{max}, of the liver. This "dotted arrow" convention is from Jacquez (1996).

Note that the fat compartment is subdivided in two subcompartments, blood and tissue, with a diffusive mass flux in between, denoted by κ. This reflects the observation that the fat compartment is rather diffusion rate than flow rate limited (Derks *et al.*, 1993).

The model contains a submodel for B(a)P metabolites. B(a)P metabolites are exclusivily formed in the liver. In the liver the formation of B(a)P metabolites leads to DNA adducts. From the liver metabolites may enter the blood. As their parent B(a)P metabolites may enter the adipose tissue, the slowly perfused and the richly perfused organs form the blood.

2.2. Model parameterization

Model parameters for compartmental volumes and blood flows are as in Zeilmaker *et al.* (1997).

B(a)P is highly lipophilic, comparable to, e.g., TCDD (log K_{ow}) = about 6; see references in Mackay *et al.* (1992)). Several papers in the literature report the application of QSARs, mainly based on the log(K_{ow}), for estimating the partition coefficient of an organic chemical; see, e.g., Poulin and Krishnan (1995) and DeJongh *et al.* (1997[a]) and references therein. A similar QSAR approach was presented in Zeilmaker *et al.* (1997) for estimating the partition coefficients of lipophilic compounds like TCDD and B(a)P. In the latter approach the partition coefficients for B(a)P and TCDD are almost the same.

In general no quantitative data are available on the relative contribution of various P450 enzymes to the metabolism of B(a)P in the rat liver, i.e. basal and inducible protein levels, dissociation constants for the binding of B(a)P to metabolising proteins and specific metabolic rate constants are usually unknown. In fact only basal and inducible concentrations of the P450 proteins 1A1 and 1A2 are available. For this reason B(a)P metabolism was initially modeled as a 1A1 and 1A2 mediated mechanism with dissociation constants for the binding of B(a)P and the specific metabolic rates of both enzymes being equal (for final modeling of B(a)P metabolism, see paragraph 2.3.5).

2.3. Model calibration: RIVM studies in the rat

The PBPK model depicted in Figure 1 contains quite a few unknown parameters. These parameters characterise the distribution of B(a)P from the blood to the organs (partition coefficients, P_i), parameters for the metabolism of B(a)P in the liver (V_{max}; K_m), the absorption half-life of B(a)P from the gastro-intestinal tract ($t_{1/2,abs}$), the fraction of orally administered B(a)P which is absorbed (F_{abs}), the parameters which characterise the induction of B(a)P metabolism after repeated exposure ($K_{d,LA}$ and $K_{d,LAX}$) and DNA adduct formation (k_{add}). The values of these parameters were obtained by fitting the model to specific data sets. In this procedure a step by step approach was taken. Calibration was started by fitting the model to a single dose *i.v.* experiment. As in this experiment the absorption of B(a)P from the gastro-intestinal tract and the autoinduction of B(a)P metabolism are not relevant such an experiment can be used to calibrate the partition coefficients of B(a)P and the parameters which characterise its (non-induced) metabolism in the liver. Then, while keeping the deposition and metabolism parameters at their calibrated values, a single dose *p.o.* data set was used to calibrate the absorption parameters. Finally, while keeping all other parameters at their calibrated values, the parameters concerning the induction mechanism of B(a)P metabolism and DNA adduct formation were obtained from repeated-administration *p.o.* experiments.

As a calibration tool the SIMUSOLV/ACSL package version 2.0 was used (Steiner *et al.* 1990).

2.3.1. Calibration of partition coefficients and non-induced metabolism parameters (P_i; V_{max}; K_M)

In Lusthof *et al.* (1993) four different *i.v.* doses have been administrated in a single dose: 0.1, 0.2, 1 and 5 mg B(a)P/kg body weight, respectively. Because of its simple and direct way of administering a single dose of B(a)P this experiment is well suited for the calibration of B(a)P partition coefficients and (non-induced) metabolism parameters. Model calibation was started by trying to explain experimental data from the 0.1, 0.2 and 1 mg/kg administered dose experiments with a linear metabolism rate. Starting with the parameterization of the partition coefficients from Zeilmaker *et al.* (1997) for TCDD (see Table 1 for the most important slowly perfused tissue-blood, P_s, and fat-blood, P_f, PC's) and several guesses for the first order elimination parameter, it was soon observed that this does not lead to a satisfactory explanation of the data (see Figure 2).

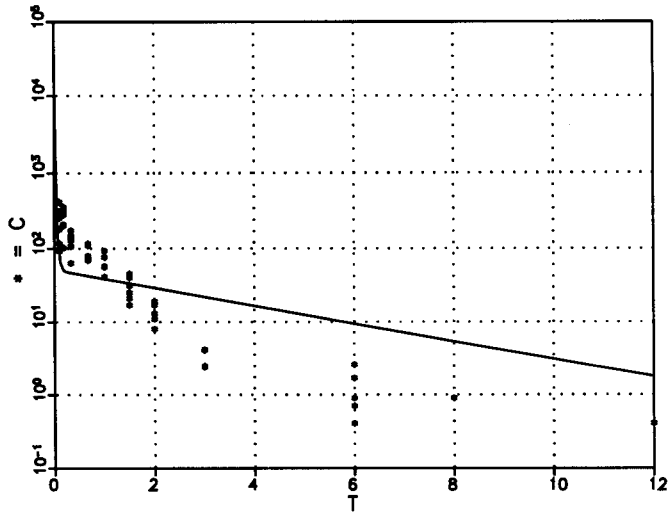

Figure 2. B(a)P concentration [nM] versus time [h]
Solid line: model; asterisks: measurements; dose: 1 [mg/kg]

For a more satisfactory explanation, the partition coefficients for the slowly perfused and fat compartment had to be reduced (see Table 1 and Figure 3).

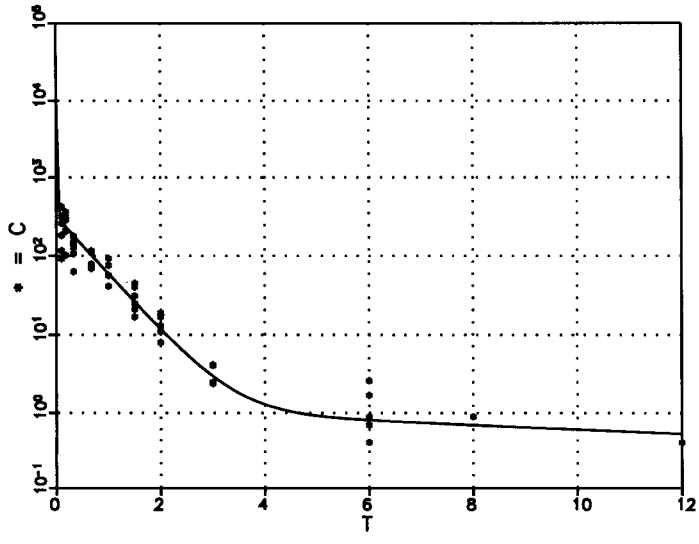

Figure 3. B(a)P concentration [nM] versus time [h]
Solid line: model; asterisks: measurements; dose: 1 [mg/kg]

The partition coefficients found (P_s = 1-3; P_f = 24-72) agree well with those reported by Wiersma and Roth (1983[b]). These authors report tissue and blood concentrations that were obtained 5 hours after the administration of 30 mg (3 mCi)/kg ^{3}H-labelled B(a)P *i.a.* From the tissue/blood ratio of these concentrations the tissue distribution is estimated under the assumption that after 5 hours the concentration distribution of B(a)P was in its terminal elimination phase. See Table 1.

Table 1. Different values found for tissue/blood distribution. P_s slowly perfused tissue-blood partition coefficient, P_f adipose tissue-blood partition coefficient.

	P_s	P_f
Zeilmaker *et al.* (1997) TCDD	12.5	630
Wiersma and Roth (1983[b]) B(a)P	7	30
This report B(a)P	1-3	24-72

The experimental data of the three lowest dose levels, i.e. 0.1, 0.2 and 1 mg/kg could be well explained by assuming linear B(a)P metabolism ($K_{met} = V_{max}/K_m$ = 26 [l/h]). However, simulations were rather sensitive for the parameter for slowly perfused tissue/blood distribution. This parameter had to be varied from 1 (dose 0.1 mg/kg), via 1.3 (dose 0.2 mg/kg) to 2 (dose 1 mg/kg). This, together with the substantial deviation of the partition coefficient values from the values found in Zeilmaker *et al.* (1997), suggests possible saturable binding of B(a)P to plasma proteins and/or blood cells. Such binding of B(a)P, notably to low- and very low density lipoproteins has been reported by Vauhkonen *et al.* (1980). However, the elucidation of this problem needs further research.

To model the highest administered dose (5 mg/kg) non-linear Michaelis-Menten metabolism kinetics was used to account for saturation. No satisfactory explanation could be found using linear metabolism kinetics. As Michaelis-Menten kinetics is also applicable for explaining the low dose data, these low dose data too were used for calibration. Partition coefficients found for the 1 mg/kg dose were used as reference and a multiplication factor was introduced for all the compartmental partition coefficients. This multiplication factor is the ratio of the partition coefficients for slowly perfused tissue in the preceding paragraph (.5 for the .1 mg/kg dose, .65 for the .2 mg/kg dose, 1 for the 1 mg/kg dose and 1.5 (initial estimate) for the 5 mg/kg dose respectively). When a mechanism of saturable plasma binding exists, one would expect the compartmental partition coefficients to increase with increasing saturation, so this procedure may be interpreted as to compensate for a possible saturable binding mechanism. The Michaelis-Menten parameters were calibrated on all data, i.e. the 0.1, 0.2, 1 and 5 mg/kg administration, and solely on the 5 mg/kg data only. Calibrating on all data, $V_{max} = 3060\,[\text{nmol / h}]$, $K_M = 8.1\,[\text{nM}]$ was found, and using the 5 mg/kg data $V_{max} = 2840\,[\text{nmol / h}]$, $K_M = 9.1\,[\text{nM}]$. Note that the value for V_{max} / K_M exceeds the previously mentioned value of K_{met} of 26 l/h by a factor more than 10. This indicates that in the analysed experiments the terminal elimination rate is flow limited, rather then intrinsic liver-metabolism rate limited.

2.3.2. Verification of partition coefficients and (non-induced) metabolism parameters and calibration of absorption parameters ($t_{1/2,abs}$; F_{abs})

The calibration of the partition coefficients and the (non-induced) metabolism mentioned in the previous paragraph was verified on the following experiment. In Klaassen *et al.* (1996) twelve rats, six males and six females, were subjected to three different treatments: 1. intravenous administration of 2 mg B(a)P/kg body weight (housing in animal cages with wire floor), 2. *idem* but instead of administration *i.v.* administration of 30 mg/kg *p.o.*, and 3. as 2. but housing in macrolon cages with middle size saw instead of wire floor. During all treatments the rats were fed *ad libitum*. As in the experiment above only male rat data were used for verification and calibration. The data of the experiment under 1. was used to verify the parameters mentioned above. The data of the experiments under 2. and 3. were used to calibrate the B(a)P absorption parameters.

First the *i.v.* data were used as a verification for the parameter values found in 2.3.1. The verification gave moderate results. It appeared that the multiplication factor for the partition coefficients introduced in 2.3.1 had to be set to 1.5, the same as for the 5 mg/kg dose in 2.3.1, and that the value for V_{max} should be more than halved with respect to the value in 2.3.1 in order to get a more reasonable result: $V_{max} = 1260$ [nmol/h]. This recalibrated parameter value was used in modeling the *p.o.* (see below) and the repeated exposure studies (see 2.3.3).

Using the same parameters found for the *i.v.* data, both the intestinal absorption fraction and the absorption rate constant were calibrated on the *p.o.* data. As there was no significant difference between the experimental data of the two different treatments (Klaassen *et al.*, 1996), the data from both experiments were combined and the absorption rate and fraction were calibrated to the median concentration values at each time point. The median concentration was chosen because this statistical parameter is less sensitive to outlyers than the mean. The absorption fraction appeared to be low, only 15%, with an absorption half-life of about one hour. Both parameters are rather sensitive, i.e., small variations cause great deviations in the simulation result. Absorption fraction and absorption half-life are also highly correlated, with a negative correlation coefficient of about 0.95.

It was noted that the concentration values observed at 6 and 8 hours after administration were about tenfold the calculated values (see Figure 4). As a matter of fact, such a phenomenon, i.e. an apparent elevated level of the venous concentration four to six hours after the peak concentration compared to model calculations, was also observed for the oral administration experiments in Lusthof *et al.* (1993) (not reported) and Olling *et al.* (1995) (see section 2.3.3).

The high 6 and 8 hour values might be explained by the uptake process. Uptake from the gastro-intestinal tract is modelled by an exponential relation, i.e., after entering the small intestine after a time interval representing passage through the stomach, the amount per unit of time taken up is proportional to the amount that is left in the intestine. However, the observations show that such a model for absorption of B(a)P from the gut content may be too simple. One should keep in mind that the animals were fed *ad libitum* and interactions within the GI-tract between food and the administrated amount of B(a)P may have influenced absorption kinetics. Also, rats, in contrast to man, possess a physiologically functional *caecum*, for storage and digestion of dietary fibers. This second digestion process could be the cause of a second, intestinal release of B(a)P followed by its absorption. Other possible explanations for the observed phenomenon are the enterohepatic recycling of B(a)P itself or the lymphatic uptake,

instead of uptake via the vena porta, of B(a)P. With regard to the enterohepatic cycle of B(a)P, the fast liver metabolism and small absorption fraction of B(a)P do not make this possibility very probable. Furthermore, also a PBPK model in which B(a)P enters the body via the lymphe, and not via the vena porta, cannot describe the phenomenon depicted in Figure 4 (dat not shown).

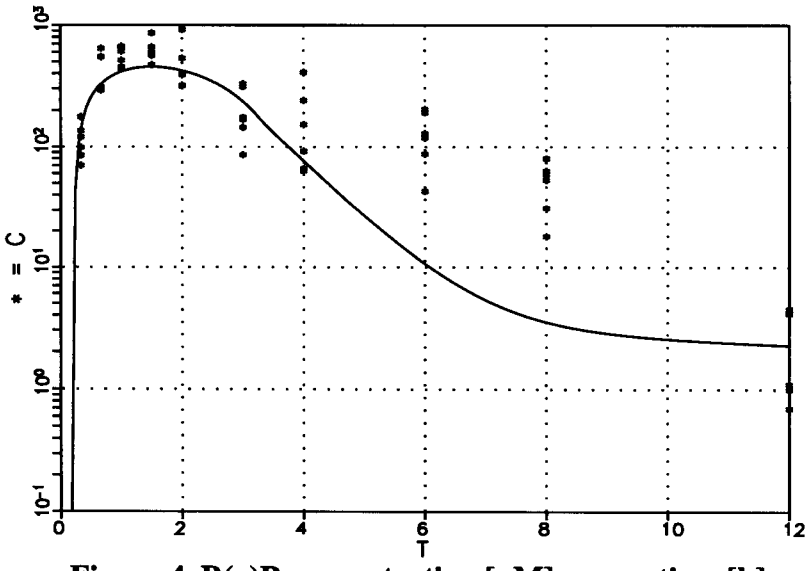

Figure 4. B(a)P concentration [nM] versus time [h]
Straight line: model; asterisks: measurements; dose: 30 [mg/kg]

2.3.3. Calibration of parameters of the autoinduction of B(a)P metabolism ($K_{d,LAX}$;$K_{d,LA}$)

Given values for the parameters characterising the distribution of B(a)P in the body, its non-induced metabolism and its absorption from the gastro-intestinal tract the parameters which refer to the auto-induction of the metabolism of B(a)P and DNA adduct formation after repeated exposure are still unknown. The parameters for the autoinduction of B(a)P metabolism were calibrated on an experiment involving the repeated exposure to B(a)P. In this experiment, reported by Olling *et al.* (1995), B(a)P was administered once daily (30 mg/kg) by gavage to 12 male and 12 female Riv:TOX rats for two weeks. Administration was on the five consecutive working days in the form of a solution in soy oil. Blood samples were taken over a period of 12 hours on the first day of administration (day 1) and on day 12 (Friday second week) from six of the animals and on day 5 (Friday first week) and day 15 (just after the weekend) from the other six. The results clearly showed autoinduction of B(a)P metabolism: maximum plasma concentrations C_{max} of B(a)P decreased after repeated administration. As in the preceding sections, only male data were used for model calibration.

First of all, the concentration data on day one were used for verification of calibrated parameters obtained in the preceding section 2.3.2. A good result was obtained (not shown). An even better result was obtained when the absorption rate was slightly decreased from 0.69 [-/h] to 0.63 [-/h].

In Zeilmaker *et al.* (1998) it is argued that once a ligand-Ah-receptor-XRE complex has been formed, the post-transcription process, i.e. the formation of P450 enzymes is likely to be independent of biological species and chemical ligand. So, the cause of the induction level overestimation was explored in the dissociation constants that determine binding of B(a)P to the Ah-receptor, $K_{D,LA}$, and the binding of the B(a)P-Ah-receptor complex to an XRE, $K_{D,LAX}$. Setting $K_{D,LA} = 82$ [nM] and $K_{D,LAX} = 4.3$ [nM] gave rather reasonable results with respect to the C_{max} level, but not for the value of t_{max} on both Fridays. See Figures 5[a,b,c,d,e].

The observed increase of t_{max} during repeated dosing could could not be explained by the PBPK model. The time it takes to reach maximum concentration, t_{max}, should decrease because of induction, where the metabolism rate increases and the absorption rate is constant. In contrast, the experiments show an apparent increase of t_{max} being 1.5 hour at the first day of administration, via 2 hours for the last Monday, to 2.5-3 hours for the administration on Friday. No explanation for this phenomenon has been found yet.

2.3.4. Calibration of P450 1A1 and 1A2 related EROD activity in the liver

In the PBPK model the enzymes P450 1A1 and P450 1A2 are responsible for the basal and the induced metabolism of B(a)P in the liver. Regarding the induction of B(a)P metabolism after repeated exposure, this induction leads to an accelerated removal of B(a)P from the body. Experimentally such removal can be observed by a lowering of C_{max} of B(a)P in the blood after repeated exposure (see foregoing paragraph). Another way of observing the induction of B(a)P metabolism is by monitoring an enzymatic activity which is characteristic of the B(a)P metabolising enzymes 1A1 and 1A2. The enzymatic activity ethoxyresorufin-o-dealkylase (EROD) is such an activity. In the PBPK model a simple model relates the P450 enzyme concentrations of 1A1, C_{1A1} and 1A2, C_{1A2}, in the liver to predicted EROD activity:

$$EROD = \beta\left(C_{1A1}(t) + \gamma \cdot C_{1A2}(t)\right)$$

(note that the time-course of the concentrations of 1A1 and 1A2 in the liver after repeated exposure is predicted by the model calibrated in 2.3.3). The coefficient β was calibrated by fitting the model to an experimental data set of induced EROD activity after repeated exposure to B(a)P. The EROD data used for this calibration were obtained from the following study. In a liver enzyme-induction range-finding study, five groups of 10 male and five groups of 10 female Riv:TOX rats were administered B(a)P for 5 weeks on the five successive working days per week. The different male and female groups received a dose of 0 (control), 1.5, 5, 15 and 50 mg/kg respectively. During the sixth week, each day two animals from each group were sacrificed and EROD activity [nmol/min/gr protein] was determined. At the day of sacrificing, the animals to be sacrificed did not receive a dose. The results were not published yet. Only the data of the male animals will be considered.

Because cross-linking of 1A2 damps EROD activity levels too much it was necessary to take $\gamma = 0$ in order to describe the B(a)P induced EROD data in the above mentioned study. So, the modeled EROD activity is proportional to the 1A1 level. Besides, it was also necessary to recalibrate the parameters $K_{D,LA}$ and $K_{D,LAX}$ from their values of 82 nM and 4.3 nM (see foregoing paragraph) to $K_{D,LA} = 18.9$ and $K_{D,LAX} = 0.96$ [nM] in order to obtain at least a crude explanation of the observed EROD activity. See Figure 6[a,b,c,d] and note the different scales, ranging from 1000 in figure 6[a] to 8000 in figure 6[d].

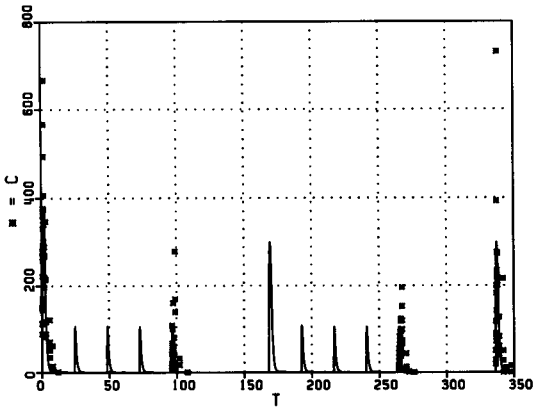

Figure 5[a] Total view

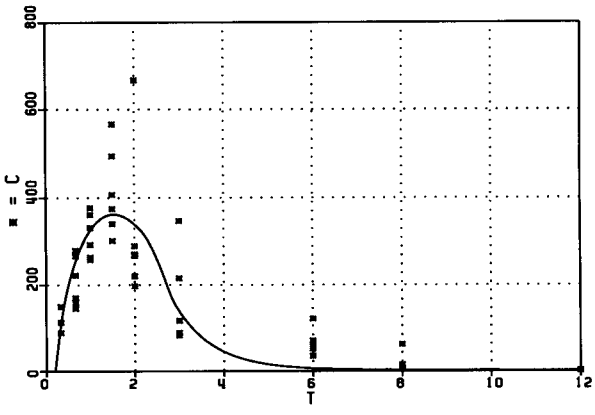

Figure 5[b] First Monday

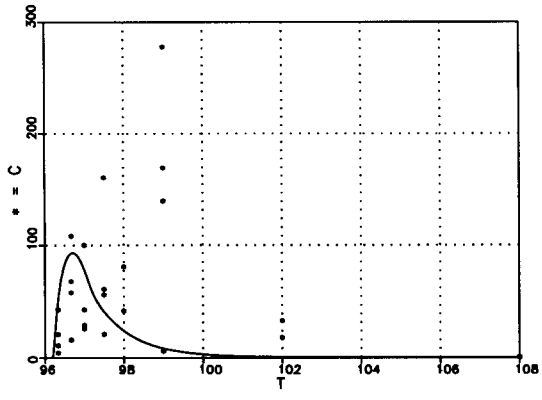

Figure 5[c] First Friday

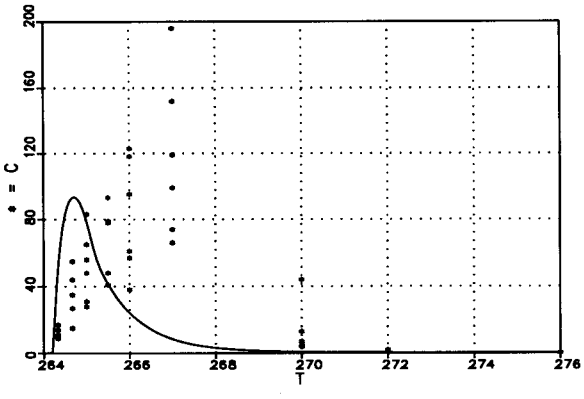

Figure 5[d] Last Friday

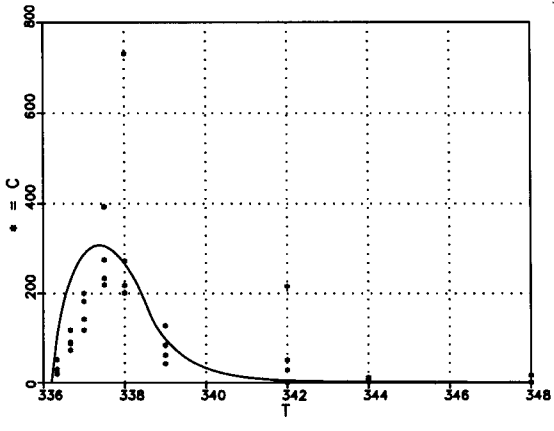

Figure 5[e] Last Monday
Daily dosing during 2 weeks; dose: 30 [mg/kg]

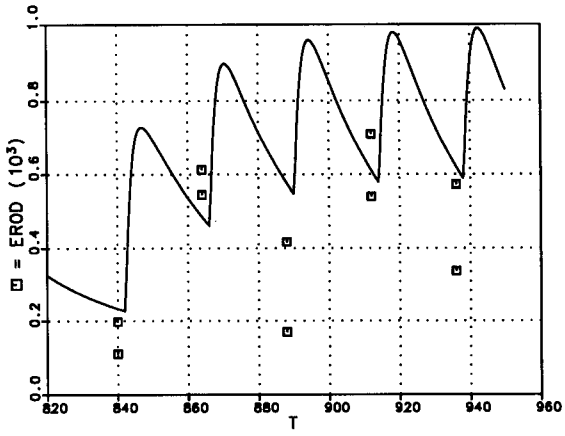

Figure 6[a] EROD versus time
Dose = 1.5 mg/kg

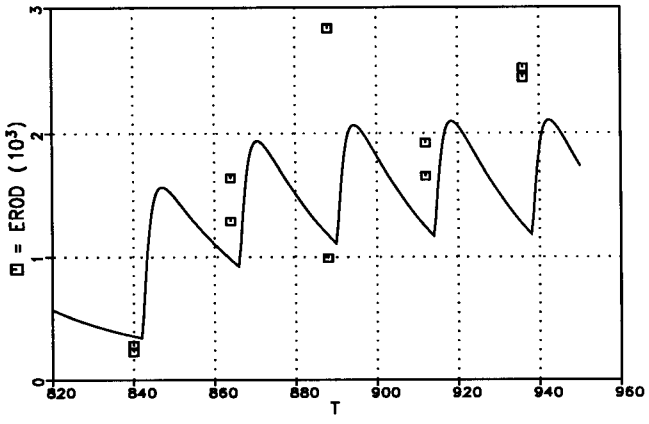

Figure 6[b] EROD versus time
Dose = 5 mg/kg

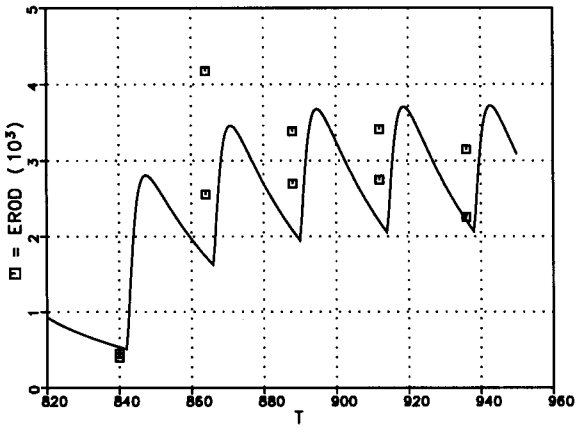

Figure 6[c] EROD versus time
Dose = 15 mg/kg

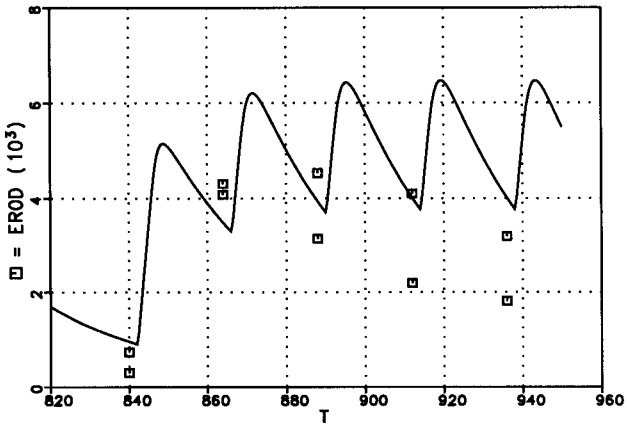

Figure 6[d] EROD versus time
Dose = 50 mg/kg

2.3.5. Calibration of induced B(a)P metabolism using both plasma kinetics of B(a)P and B(a)P induced EROD activity in the liver

In paragraph 2.3.3 plasma kinetic data of B(a)P were used to calibrate the autoinduction of B(a)P metabolism. For this calibration a PBPK model was used in which both 1A1 and 1A2 contribute to the metabolism of B(a)P. In paragraph 2.3.4 B(a)P induced 1A1 and 1A2 related EROD activity was calibrated. Here it was found that the induction of EROD activity could only be described with a PBPK model in which this activity is exclusivily related to 1A1. Furthermore the induction parameters necessary to describe the EROD induction data, i.e. $K_{d,LA}$ and $K_{d,LAX}$, lead to an a most unsatisfactory explanation of the plasma kinetic data used in paragraph 2.3.3. These observations indicate that a PBPK model which assumes an equal contribution of 1A1 and 1A2 to the metabolism of B(a)P and to EROD activity cannot, at the same time, describe the data depicted in Figures 5 and 6. Both data sets could only be described together with a PBPK model in which induced 1A1 is responsible for induced EROD activity and 1A2 almost solely for total B(a)P metabolism (note that the available data do not allow an estimation of the specific contribution of 1A1 to total B(a)P metabolism). The former condition was met by setting γ equal to 0. The latter condition was met by setting the associated specific metabolism rate of 1A1 for B(a)P (km_1) equal to 0. Finally $K_{D,LA} = 25$ and $K_{D,LAX} = 1$ were found to retain the results in figures 5 and 6.

2.3.6 Calibration of DNA adduct formation

In the PBPK model B(a)P metabolism solely occurs in the liver. Furthermore, B(a)P metabolism is thought to occur mainly via 1A2. In the model the formed B(a)P metabolites may diffuse in the blood. In the liver B(a)P metabolites may react with DNA giving rise to DNA adducts. DNA adduct formation was assumed to linearly depend on the concentration of B(a)P metabolites in the blood. From the blood the metabolites may spread over the body (see Figure 1). A submodel was used to describe the fata of B(a)P metabolites in the body (see Figure 1). Flows and volumes in this model are as in the B(a)P model itself (Fig. 1). All metabolite partition coefficients were taken to be one, except bile. An entero-hepatic recirculation efficiency for metabolites was taken to be about 22.5% (Lusthof *et al.* (1994)). The metabolite model is linear and any other choice would lead to the same hepatic concentration profile apart from a multiplication factor. DNA repair was assumed to linearly depend on the amount DNA adducts formed. Net DNA adduct formation was modeled as:

$$\frac{d}{dt}Add = k_{Add} D_h / R_h - \mu_{Add} Add$$

were Add [-] is the adduct count level, k_{Add} [-/(nM · h)] is a growth rate factor D_h [nM] is the hepatic metabolite concentration, R_h [-] is the hepatic-blood metabolite partition coefficient, so, the free metabolite hepatic concentration is D_h / R_h, and μ_{Add} [-/(nM · h)] is a DNA-adduct repair factor. The entity D_h is predicted by the B(a)P PBPK model (see paragraph 2.3.5). The parameter R_h was assumed to have a value of 1 (see above). The parameter μ_{Add} was obtained from an experiment. In this experiment rats were daily dosed for 3 weeks (5 days per week) with 5 mg B(a)P/kg body weight and adduct levels were counted on several days after dosing. The repair half-life of several adducts was estimated to be about 22 days (Kroese, pers. communication).

The parameter k_{add} was obtained by fitting the model to data from an experiment in which male rats were fed a daily oral dose of 1.5 and 15 mg/kg respectively. At day 5, 25 and 53 adduct levels in the liver of three animals were determined (unpublished results). For both the 1.5 and 15 mg/kg data sets separate, a reasonable explanation could be found. However the growth rate factor k_{Add} had to be taken a four times higher for the data from the 15 mg/kg experiment with respect to the data from the 1.5 mg/kg experiment. From section 2.3.5 note that the metabolites are modelled as if formed by the 1A2 enzymes only. If it is assumed that the level of metabolites formed by 1A1 is negligible with respect to the level formed by 1A2, but also that just these metabolites are responsible for the formation of adducts, one obtains a reasonable explanation of the data for both dosing regimes with only one value for the growth factor k_{Add} (see Figure 7[a,b], note that data differ about a factor 25, while the doses differ only a factor 10).

Also note that, as the specific metabolism rate of the 1A1-enzyme, and thus the absolute level of the 1A1-metabolite could not be estimated (see paragraph 2.3.5), the estimation of k_{Add} has no absolute meaning.

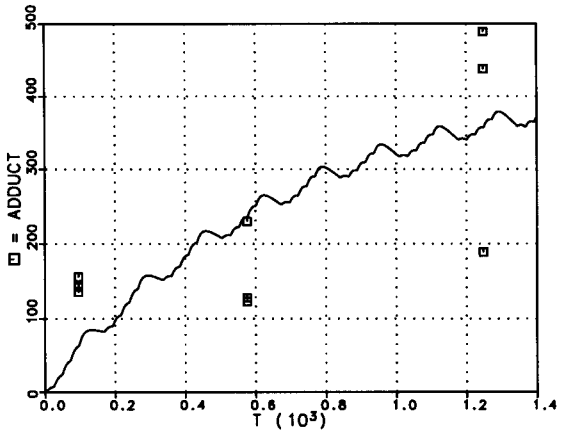

Figure 7[a] Number of adducts versus time. Dose = 1.5 mg/kg

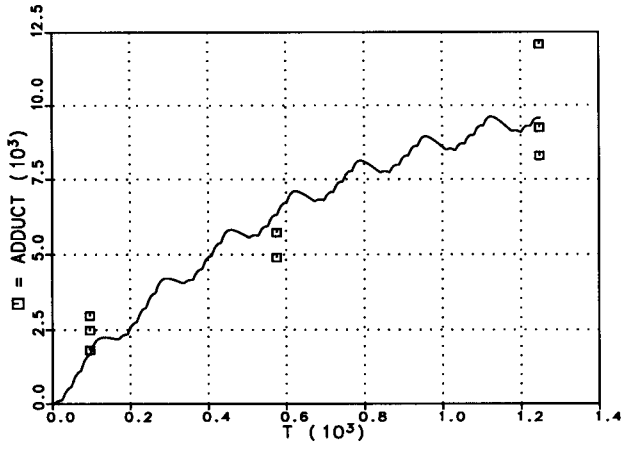

Figure 7[b] Number of adducts versus time. Dose = 15 mg/kg

2.3.7. Model calibration: Concluding remarks

In summary a PBPK of B(a)P in the rat was calibrated by fitting the model to a number of specific data sets. These sets included the uptake of B(a)P from the gastro-intestinal tract into the blood (paragraph 2.3.2), the distribution of B(a)P from the blood to the organs (paragraph 2.3.1), the auto-induction of the metabolism of B(a)P in the liver (paragraphs 2.3.3, 2.3.4 and 2.3.5) and the formation of DNA adducts in the liver after repeated exposure (paragraph 2.3.6). Under the condition that the metabolism of B(a)P mainly occurs by the P450 protein 1A2, and not 1A1, and that B(a)P induced EROD activity and DNA adduct formation are mediated by 1A1, and not 1A2, the above mentioned data sets could reasonably be described with one and the same PBPK model (see Figures 2-7).

3. RAT PBPK MODEL SIMULATIONS AND EXTRAPOLATION TO MAN

3.1. Dose dependency in the rat

The model that was found in the preceding section to be most suitable to explain B(a)P concentration levels together with EROD and DNA adduct level, has been used for simulating a daily oral dosing regime for a wide range of dose levels. The daily oral dosing regime in this simulations is not interrupted, as in the experiments, during weekends. The dose levels used ranged from 5 pg/kg to 50 mg/kg bodyweight. These simulations were carried out in order to estimate the dependency of the parent compound and metabolite concentrations as well as EROD activity and DNA adduct levels on the dose level and on the interrelation of some of these, i.e., dependency of steady-state adduct levels on 1A1-metabolite level under the model assumptions.

In the following subsections the results of these simulations will be presented graphically and briefly discussed. Because of the wide range of dose levels and its subsequential simulation outcome, all results will be presented on double log scale[1].

3.1.1. Plasma C_{max} and AUC of B(a)P

The induction of metabolism will cause a varying C_{max} and daily AUC of B(a)P. However, after a few days, these quantities will reach steady state, i.e., C_{max} and daily AUC will not vary any more. These steady state values are reported. It appears hard to predict dose dependency of these to classical kinetic parameters. Saturable metabolism will lead to an increase of both values, because relatively little B(a)P will be metabolised. Induced metabolism however will also lead to a decrease, because more enzymes capable of metabolising B(a)P will be available. From the model simulations it appears that for a wide range of dose levels, up to about 50,000 ng/kg, there is a linear relationship. See figure 8, were the result for C_{max} is shown, the result for the AUC is essentially the same. The dotted line shows the linear extrapolation of the low dose results.

3.1.2. Plasma C_{max} and daily AUC of 1A2-metabolite

As within 24 hours virtually all B(a)P is metabolised, the AUC will be proportional to the dose (see figure 9). C_{max} too appears to be almost proportional to dose level (not shown).

3.1.3. plasma C_{max} and daily AUC of 1A1-metabolite

For low doses, i.e., doses less than about 100 ng/kg, it is expected that induction is negligible and metabolism is linear. As a consequence C_{max} and AUC of the 1A1-metabolite is supposed to vary linearly with dose. In the range of higher doses the ratio of 1A1 and 1A2 levels increases and it may be expected that C_{max} and AUC for 1A1 metabolites will increase more than proportionally with dose level. From figure 10 it appears that eventually the relation between

[1]When on the linear scale a linear relation like $y = ax$ exists, i.e. a linear response through 0 with slope a, then on the double-log scale $Y = \log(y) = \log(x) + \log(a) = X + A$, i.e. the response is still linear, but goes through A and has slope 1.

dose and C_{max} is linear again, because of saturation of the metabolising process. The dotted line shows linear extrapolation of the low dose results.
The results for the AUC are essentially the same (not shown).

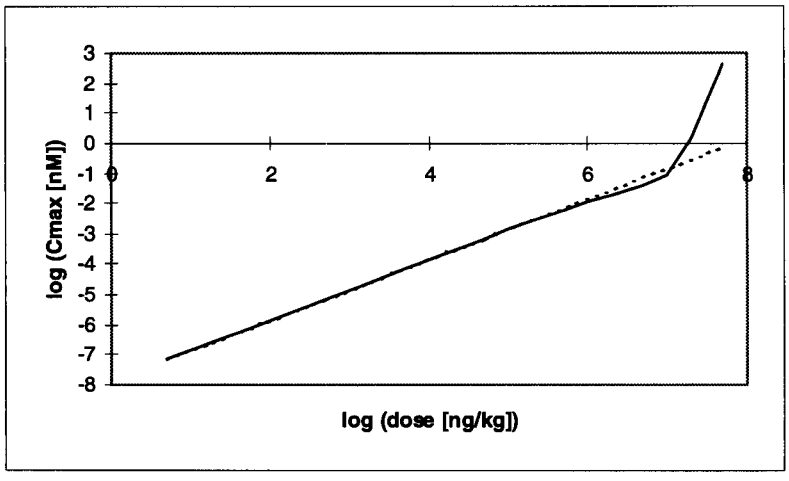

Figure 8. Daily C_{max} versus dose level.

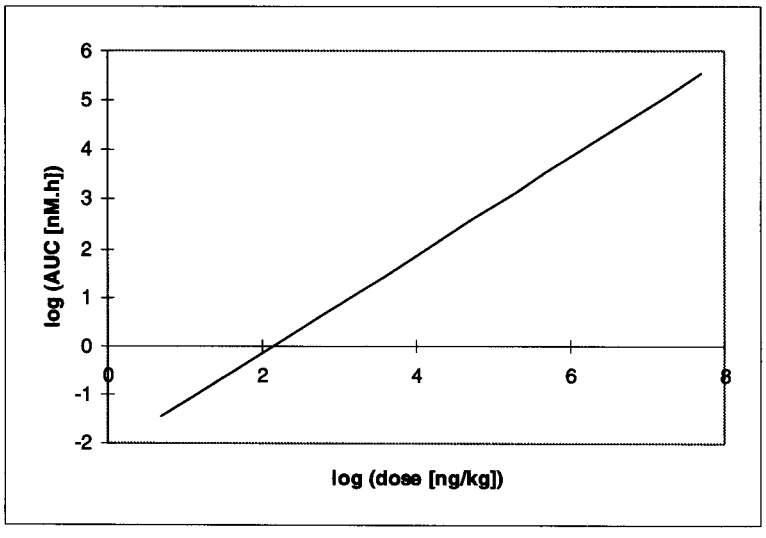

Figure 9. AUC 1A2-metabolite versus dose level

3.1.4. P450 1A1 and -1A2 enzyme levels and EROD level

In the model both B(a)P and its metabolites will never reach a plateau level. Instead, P450 enzymes and EROD do reach a non-zero plateau level. However, the actual concentrations and activity, respectively, vary around these levels. A few hours after dosing levels rise because of induction, reach their maximum and than steadily level off again. The EROD induction level is linear dependent on the 1A1 enzyme level, so only the dependencies of 1A1 and 1A2 on dose level will be shown. For the low dosing regime, these levels will be almost the base levels. See Figure 11.

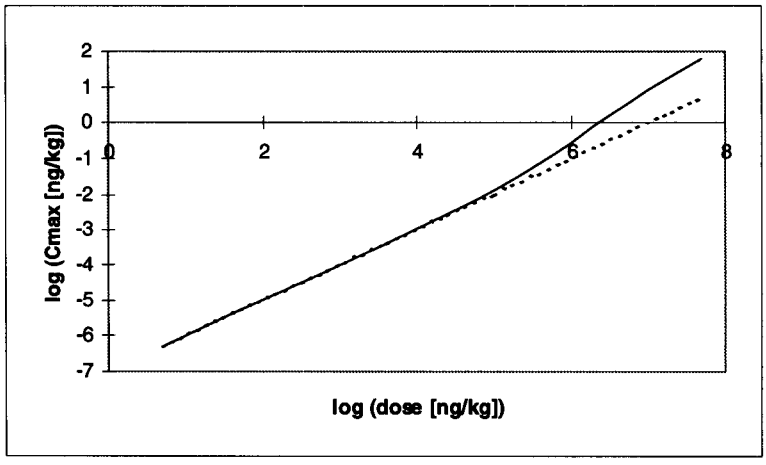

Figure 10. C_{max} 1A1-metabolite versus dose level

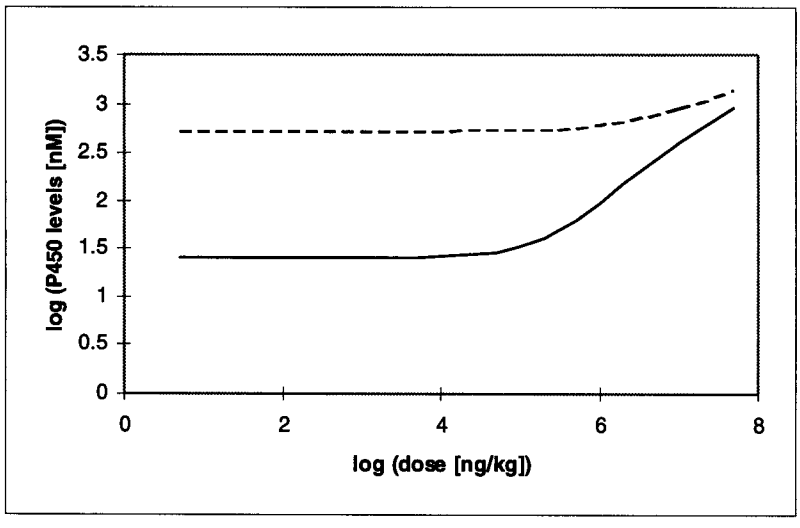

Figure 11. P450 1A1 (solid) and 1A2 (broken) concentrations versus dose level

3.1.5. DNA-adduct levels

Increasing the dose, 1A1-metabolite levels will increase and so will the DNA-adduct level. Moreover, because of the induction of 1A1 enzymes this process is amplified, and as a result an increase more than proportional to dose level is to be expected (Figure 12). This figure, compared with the dose dependency of 1A1-metabolite level in Figure 10 indicates a linear relationship between number of adducts and 1A1-metabolite level. This is confirmed in Figure 13.

For comparison, the dependence of the number of adducts on EROD activity is shown in figure 14. Because at the low dose levels EROD activity, which is linear dependent on 1A1 enzyme level, is almost constant, a marginal dependence of number of adducts is to be expected. The diamonds show the dose levels of 5, 5×10^1, 5×10^2, 5×10^3, 5×10^4, 10^5, 2×10^5, 5×10^5, 10^6, 2×10^6, 5×10^6, 10^7, 2×10^7 and 5×10^7 pg/kg going from the lower left to the upper right.

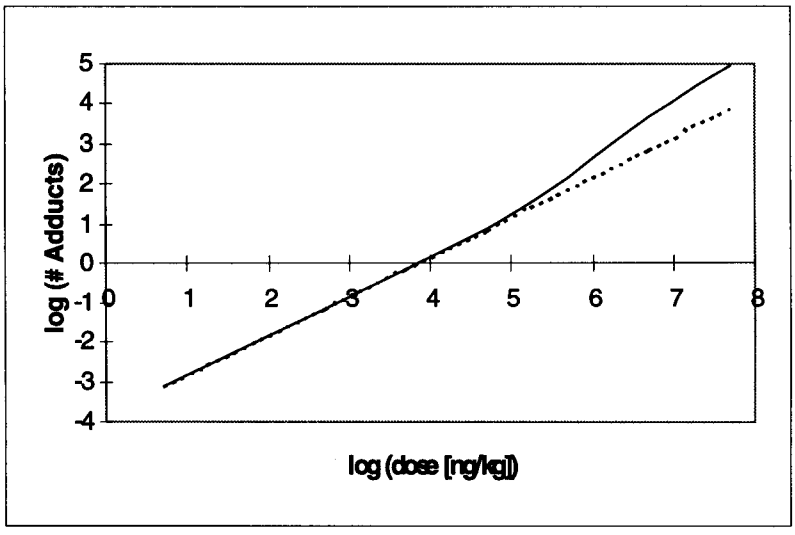

Figure 12. Number of adducts versus dose level

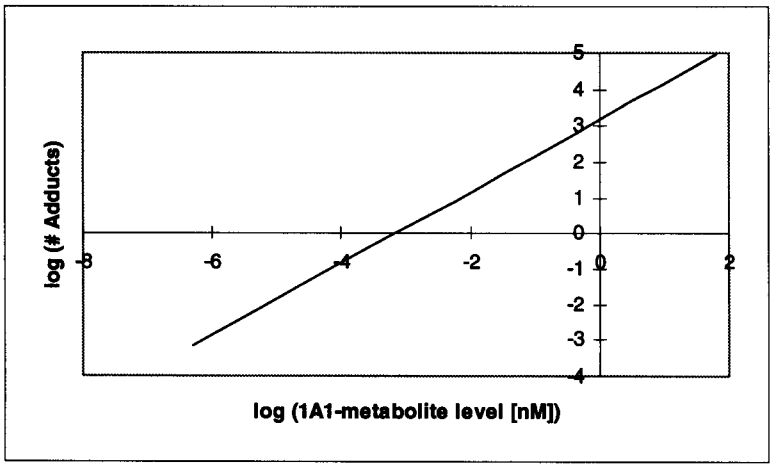

Figure 13. Number of adducts versus 1A1-metabolite level

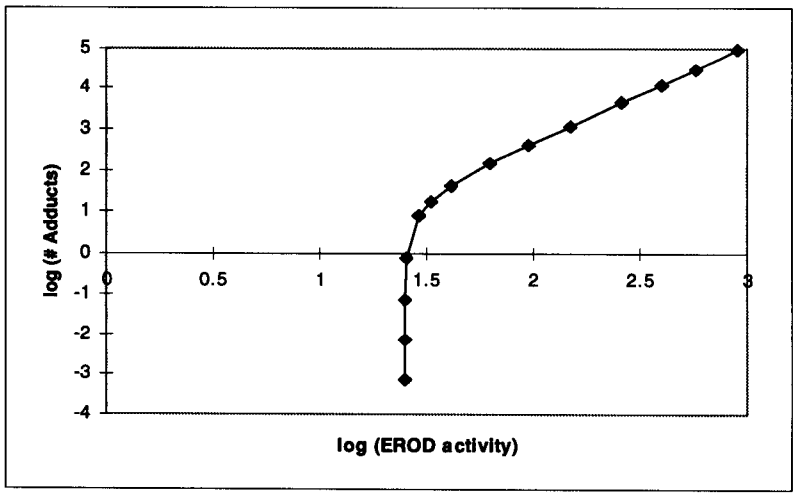

Figure 14. Number of adducts versus EROD activity

3.2. Extrapolation to man

For risk assessment, the rat model as it is introduced and calibrated should be scaled to a human model. Obviously, compartmental volumes and flows should be adjusted to the human values. Assuming the blood composition of man and rat to deviate not too much, and the lipid content of the compartmental tissues to be equal, the partition coefficients could be taken the same for man as for rat.

The main difficulty of the scaling procedure is in the scaling of B(a)P metabolism. Zeilmaker *et al.* (1998) assumed that the Ah-receptor concentration, P450 protein catabolism and the dissociation constant for ligand-P450 protein binding are the same for rat and man. However, the basal P450-1A1 and -1A2 protein concentration in man appears to be negligible (*ibid.*). Also, the dissociation constant for the binding of the ligand-receptor complex to an XRE for man is about 20 times the Ah-receptor concentration (*ibid.*). A different value for the dissociation constant of the ligand-receptor binding itself was estimated from human experimental data, but found to be of the same order as in the rat (*ibid.*).

Assuming that the differences found between human and rat parameters do not depend on the specific ligand, i.e. TCDD in Zeilmaker *et al.* (1997) and B(a)P in this report, a human PBPK model for B(a)P can be extrapolated from the rat model for B(a)P. According to the remarks in the preceding section, in this model basal 1A1 and 1A2 levels are set to 0 and the value for the ligand-receptor-XRE complex 20 times Ah receptor concentration. The value for the ligand-receptor binding dissociation constant was kept the same. Human physiologic parameters are from ILSI/RSI (1994).

Because about 95% of the daily dose of B(a)P is metabolised throughout, the total metabolite level is linear dependent on dose level, as in the rat. Because induced 1A1 and 1A2 enzyme levels are the same, in contrast to the rat where the 1A1 level increased relative to the 1A2 level, an almost linear relationship is found between dose and 1A1-metabolite level. As a consequence, as the number of adducts scales linearly with 1A1-metabolite level, the dependence of the number of adducts on dose level is linear.

4. CONCLUSIONS

Application of the model concepts of Zeilmaker *et al.* (1997) in a PBPK model for B(a)P in the rat could well explain the decrease of plasma AUC and C_{max} on Fridays and its re-increase on a Monday during the experiment in Olling *et al.* (1995). However, no explanation could be found for the experimentally found increase of t_{max} which, from a model point of view, should decrease.

In Olling et al. (1995) it was argued that perhaps B(a)P kinetics could be explained as well by some time-dependent absorption kinetics. However, this would imply a decrease in the intestinal absorption fraction of B(a)P and, consequently, a decrease in B(a)P metabolites. In this report it appears that both EROD data and DNA adduct levels favour a model where P450 enzyme induction is pertinent and disfavour a model which implies decreasing intestinal absorption.

Still, the experimental results for t_{max} as well B(a)P concentration levels 6 to 8 hours after administration show the need for a better understanding and modelling of intestinal absorption.

From the calibration of B(a)P concentration data together with EROD data and DNA-adduct data it appeared that metabolites formed by one P450 pathway, in this model the 1A1 enzyme, are a minor fraction of the total of metabolites. This total is formed almost solely by another P450 pathway, in this model the 1A2 enzyme. Nevertheless, the number of DNA-adducts could be modelled with a dose independent formation rate only, when associated solely with 1A1-metabolites. To the authors knowledge there is no literature on the relative contribution of 1A1 and 1A2 to B(a)P metabolism.

Recent unpublished experimental results on B(a)P metabolism using microsomes of rat livers that were induced by several different inducers during 3 to 10 days seems to support these assumptions in part. B(a)P was added and, amongst others, EROD and POD activity was measured as well as the velocity of formation of several B(a)P metabolites. If it is assumed that EROD activity is associated with the 1A1 enzyme and POD activity with the 1A2 enzyme, then the implications of this experiment are twofold. First, from linear regression, the formation velocity of the 7,8-OH diol, which supposedly is responsible for the formation of DNA-adducts, could be associated with the induced 1A1 concentrations and not 1A2. This observation supports our model. Secondly, also the formation velocity of the 3-OH hydroxy metabolite could only be associated with the induced 1A1 concentrations and not 1A2. This is in contradistinction to our model. However, it appeared to be absolutely impossible in our model to relate B(a)P plasma concentrations, EROD activity and DNA adduct levels to the 1A1 enzyme solely. This needs further research.

Taking the model as it is, simulations with respect to dose dependency of B(a)P concentration levels and concentrations levels of its metabolites, EROD activity levels and DNA-adducts were carried out. The main conclusion is that the number of DNA-adducts scales linearly with 1A1-metabolite concentration level.

As the 1A1-metabolite level depends non-linear on dose level, because the concentration ratio of metabolising 1A1 and 1A2 enzymes increases with increasing dose level, so the number of DNA-adducts does for the rat. However, from an extrapolation to man, it appears that the 1A1-metabolite level depends linear on dose level, because the concentration ratio of the metabolising enzymes is constant. So, in humans the number of DNA-adducts scales linearly with dose.

5. LITERATURE

Abraham, K., Krowke, R. and D. Neubert; Pharmacokinetics and biological activity of 2,3,7,8-tetrachlorodibenzo-*p*-dioxin 1. Dose-dependent tissue distribution and induction of hepatic ethoxyresofurin O-deethylase in rats following a single injection; *Arch. Toxicol.*, 62 (1988) 359-368

Chen, H.G. and J.F. Gross; Estimation of tissue-to-plasma partition coefficients used in physiological pharmacokinetic models; *J. Pharmacokin. Biopharm.* **7** (1979) 117:125

DeJongh, J., Verhaar, H.J.M., and J. Hermens; A quantitative property-property relationship (QPPR) approach to estimate tissue-blood partition coefficients of organic chemicals in rats and humans; *Arch. Toxicol.*, **72** (1997) 17:25

Derks, H.J.G.M., Berende, P.L.M., Everts, H., Olling, M., Liem, A.K.D. and A.P.J.M. de Jong; Een fysiologisch farmacokinetisch model voor 2,3,7,8-TCDD in de koe; RIVM rapport nr. 643810001, Bilthoven, The Netherlands, 1993. *In Dutch*

ILSI/RSI; *Physiological parameter values for PBPK models*; 1994

Jacquez J.A.; *Compartmental analysis in biology and medicine (Third ed.)*; BioMedware, Ann Arbor,USA, 1996

Johannessen, W.M., Tyssebotn, I.M. and J. Aarbakke; Antipyrine and acetaminophen kinetics in the rat: comparison of data based on blood samples from the cut tail and a cannulated femoral artery; *J. Pharm. Sciences* **71** (1982) 1352-1356

Klaassen, R., Olling, M. en K.J. Lusthof; De invloed van zaagselbodem- of draadbodemkooien op de kinetiek van oraal toegediend benzo(a)pyreen bij de rat; RIVM rapport nr. 658603006, Bilthoven, The Netherlands, 1993. *In Dutch.*

Kociba, R.J., Keyes, G.G., Beyer, J.E., Carreon, R.M., Wade, C.E., Dittenber, D.A.,Kalnis, R.P., Frauson, L.E., Park, C.N., Barnard, S.D., Hummel, R.A. and C.G. Humoston; Results of a two-year chronic toxicity and oncogenicity study of 2,3,7,8-Tetrachlorodibenzo-*p*-dioxin in rats; *Toxicol. Appl. Pharmacol.* **46** (1978) 279-303

Leung, H.W., Paustenbach, D.J., Murray, F.J. and M.E. Andersen; A physiological pharmacokinetic description of the tissue distribution and enzyme inducing properties of 2,3,7,8-tetrachlorodibenzo-*p*-dioxin in the rat; *Toxicol. Appl. Pharmacol.*, **103** (1990[a]) 399-410

Leung, H.W., Poland, A., Paustenbach, D.J., Murray, F.J. and M.E. Andersen; Pharmacokinetics of [^{125}I]-2-iodo-3,7,8-trichlorodibenzo-*p*-dioxin in mice: Analysis with a physiological modeling approach; *Toxicol. Appl. Pharmacol.*, **103** (1990[a]) 411-419

Lusthof, K.J., Olling, M., Kroese, E.D., Beenen, J., Poelen, M.J., Vaessen, H.A.M.G. and C.G. van de Kamp; Farmacokinetiek en biologische beschikbaarheid van benzo(a)pyreen B(a)P in de RIV:tox rat; RIVM rapport nr. 658603002, Bilthoven, The Netherlands, 1993. *In Dutch.*

Lusthof, K.J., Groen, C., Olling, M., en E.D. Kroese; Excretie van radioactiviteit in de gal en urine van de Riv:TOX rat na intraveneuze toediening van ^{14}C-gelabeld benzo(a)pyreen en reabsorptie van radioactiviteit uit de gal; RIVM rapport nr. 658603003, Bilthoven, The Netherlands, 1994. *In Dutch.*

Lusthof, K.J., Olling, M., en E.D.; Plasmaspiegels van bezo(a)pyreen na viereneenhalve maand herhaalde orale toediening (5 dagen/week) van benzo(a)pyreen aan de Riv:TOX rat; RIVM rapport nr. 658603005, Bilthoven, The Netherlands, 1996. *In Dutch.*

Moolgavkar, S.H., Dewanji, A., and D.J. Venzon; A stochastic two-stage model for cancer risk assessment. I. The hazard function and the probability of tumor; *Risk Analysis*, **8** (1988) 383-392

Mackay, D., Shiu, W.Y. and K.C. Ma; *Illustrated handbook of physical-chemical properties and environmental fate for organic chemicals, vol. II*; Lewis Publishers, Chelsea, Mich., USA, 1992

Olling, M., Lusthof, K.J., Kroese, E.D., Beenen, J., Poelen, M.J. en R. Klaassen; Toxicokinetiek van benzo(a)pyreen bij de Riv:TOX rat na herhaalde orale toediening; RIVM report nr. 658603004, Bilthoven, The Netherlands, 1995. *In Dutch.*

Parham, F.M., Kohn, M.C., Matthews, H.B., Drosa, C. and C.J. Portier; *Using structural information to create physiologically based pharmacokinetic models for all polychlorinated biphenyls.* I *Tissue:blood partition coefficients*; Toxicol. Appl. Pharmacol., **144** (1997) 340-347

Poulin, P. and K. Krishnan; A biologically-based algorithm for predicting human tissue:blood partition coefficients of organic chemicals; *Hum. Exp. Toxicol.*, **4** (1995) 273-280

Roth, R.A. and A. Vinegar; Action by the lungs on circulating xenobiotic agents, with a case study of physiologically based pharmacokinetic modeling of benzo(a)pyrene disposition; *Pharmac. Ther.*, **48** (1990) 143-155

Tritscher, A.M., Goldstein, J.A., Portier, C.J., McCoy, Z., Clark, G.C. and G.W. Lucier; Dose-response relationships for chronic exposure to 2,3,7,8-Tetrachloro-dibenzo-*p*-dioxin in a rat tumor promotion model: quantification and immunolocalizatio of CYP1A1 and CYP1A2 in the liver; *Cancer Research*, **52** (1992) 3435-3442

Vauhkonen, M., Kuusi, T. and P.K.J. Kinnunen; Serum and tissue distribution of Banzo[a]pyrene from intravenously injected chylomicrons in rat in vivo; *Cancer Letters*, **11** (1980) 113-119

Wiersma D.A. and A. Roth; The prediction of benzo(a)pyrene clearance by rat liver and lung from enzyme kinetic data; *Molecular Pharmac.*, **24** (1983[a]) 300-308

Wiersma D.A. and A. Roth; Total body clearance of circulating benzo(a)pyrene in concious rats: effect op pretreatment with 3-methylcholanthrene and the role of liver and lung; *J. Pharmacol. Exp. Ther.*, **226** (1983[b]) 661-667

Zeilmaker, M.J., and J.C.H. van Eijkeren; Modeling of Ah-receptor dependent P450 induction I. Cellular model definition and its corporation in a PBPK model of 2,3,7,8-TCDD; *RIVM report nr 604138.001*, Bilthoven, The Netherlands, 1997

Zeilmaker, M.J., and J.C.H. van Eijkeren; Modeling of Ah-receptor dependent P450 induction II. Simulating P450 in rat; *RIVM report nr 604138.002*, Bilthoven, The Netherlands, 1998